

Reversible binding of water, methanol, and ethanol to a five-coordinate ruthenium(II) complex†

Erin S. F. Ma, Brian O. Patrick and Brian R. James*

Department of Chemistry, University of British Columbia, Vancouver, British Columbia, Canada, V6T 1Z. E-mail: brj@chem.ubc.ca

SUPPLEMENTARY MATERIAL

Figures S1–S11Pages 3–9

Figure S1. ORTEP diagram of *trans*-RuCl₂(P–N)(P(*p*-tolyl)₃)(H₂O) (**2b**) with 50% probability thermal ellipsoids.

Figure S2. TGA spectrum of **2a**, depicting the loss of acetone and H₂O from 80 to 110 °C.

Figure S3. ³¹P{¹H} NMR spectra (202.5 MHz) of *trans*-RuCl₂(P–N)(PPh₃)(H₂O) (**2a**) in CD₂Cl₂ at various temperatures. An unidentified, trace species is seen at δ49.8 and δ59.0 from –50 to –80 °C .

Figure S4. ³¹P{¹H} NMR spectra (121.4 MHz, 20 °C) of RuCl₂(P–N)(PPh₃) (**1a**) in *d*₆-acetone with added H₂O to form **2a**.

Figure S5. ¹H NMR spectra (500 MHz) of *trans*-RuCl₂(P–N)(PPh₃)(H₂O) (**2a**) in CD₂Cl₂ at various temperatures.

Figure S6. Spectral changes observed upon addition of H₂O to RuCl₂(P–N)(PPh₃) (**1a**) (1.21 × 10^{–3} M) in C₆H₆ at 25 °C. Added [H₂O] = (a) 0.0, (b) 0.0056, (c) 0.0111, (d) 0.0222, (e) 0.0333, (f) 0.0444, (g) 0.0776 M.

Figure S7. Spectral changes observed upon addition of H₂O to RuCl₂(P–N)(PPh₃) (**1a**) (1.12 × 10^{–3} M) in acetone at 25 °C. Added [H₂O] = (a) 0.0, (b) 0.0089, (c) 0.2652, (d) 0.9171, (e) 1.9702, (f) 3.9591 M.

Figure S8. Spectral changes observed upon addition of H₂O to RuCl₂(P–N)(PPh₃) (**1a**) (1.19 × 10^{–3} M) in THF at 25 °C. Added [H₂O] = (a) 0.0, (b) 0.0444, (c) 0.1110, (d) 0.2220, (e) 0.9992, (f) 4.330 M.

Figure S9. Determination of K for reversible binding of H₂O to **1a** at 25 °C.

Concentrations obtained by absorbance at 678 nm (Fig. 4). Data at higher [H₂O] omitted due to solubility limit of H₂O in CH₂Cl₂: 0.128 M at 25 °C (IUPAC Solubility Data Series, Vol. 60, *Halogenated Methanes with Water*; A. L. Horváth, F. W. Getzen, eds.; Oxford Univ. Press: Oxford, 1995, p. 153).

Figure S10. ¹H NMR spectrum (300 MHz) of *trans*-RuCl₂(P–N)(PPh₃)(MeOH) (**3**) in CD₂Cl₂ at room temperature.

Figure S11. DSC curves for the *trans*-RuCl₂(P–N)(PR₃)(H₂O) complexes **2a** (R = Ph) and **2b** (R = *p*-tolyl).

Table S1. ³¹P{¹H} NMR data for RuCl₂(P–N)(PPh₃) (**1a**) and *trans*-RuCl₂(P–N)(PPh₃)(H₂O) (**2a**) in various solvents at 20 °C.Page 10

Appendix A. Crystal data for *trans*-RuCl₂(P–N)(P(*p*-tolyl)₃)(H₂O) (**2b**).Pages 10–21

Appendix B. Thermodynamic calculations and UV-Vis spectroscopic data for the reversible formation of *trans*-RuCl₂(P–N)(PR₃)(H₂O).Pages 22–29

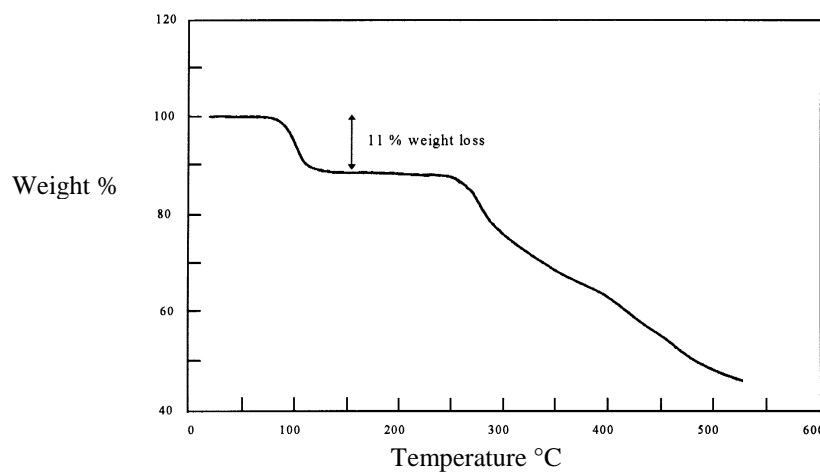


Fig S1 TGA spectrum of **2a**, depicting the loss of acetone and H₂O from 80 to 110 °C.

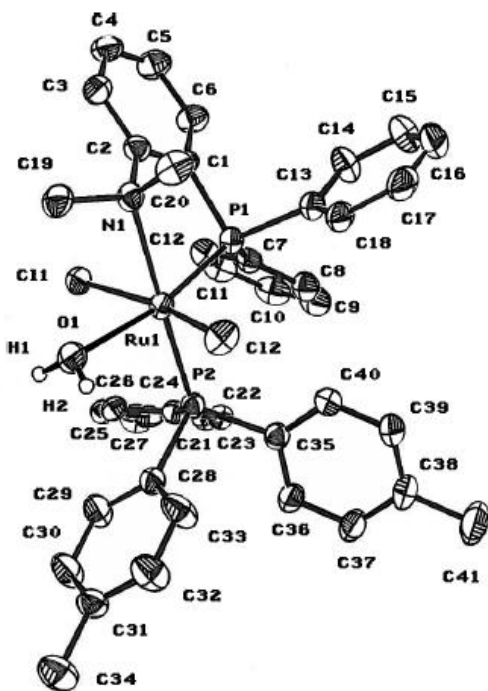


Fig S2 ORTEP diagram of *trans*-RuCl₂(P-N)(P(*p*-tolyl)₃)(OH₂) (2b) with 50% probability thermal ellipsoids.

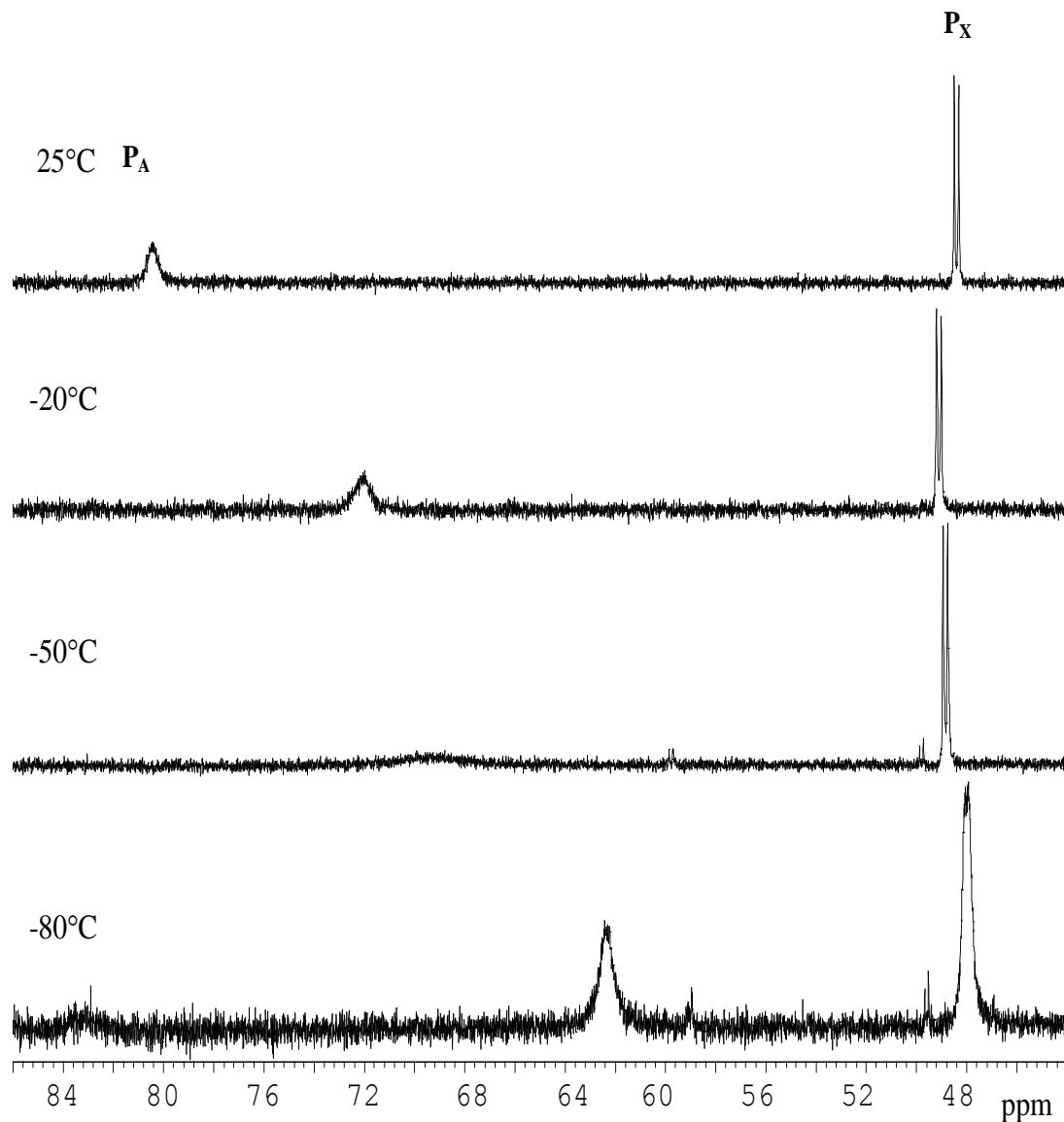


Fig S3 $^{31}\text{P}\{\text{H}\}$ NMR spectra (202.5 MHz) of *trans*-RuCl₂(P–N)(PPh₃)(H₂O) (**2a**) in CD₂Cl₂ at various temperatures. An unidentified, trace species is seen at δ 49.8 and δ 59.0 from -50 to -80 °C.

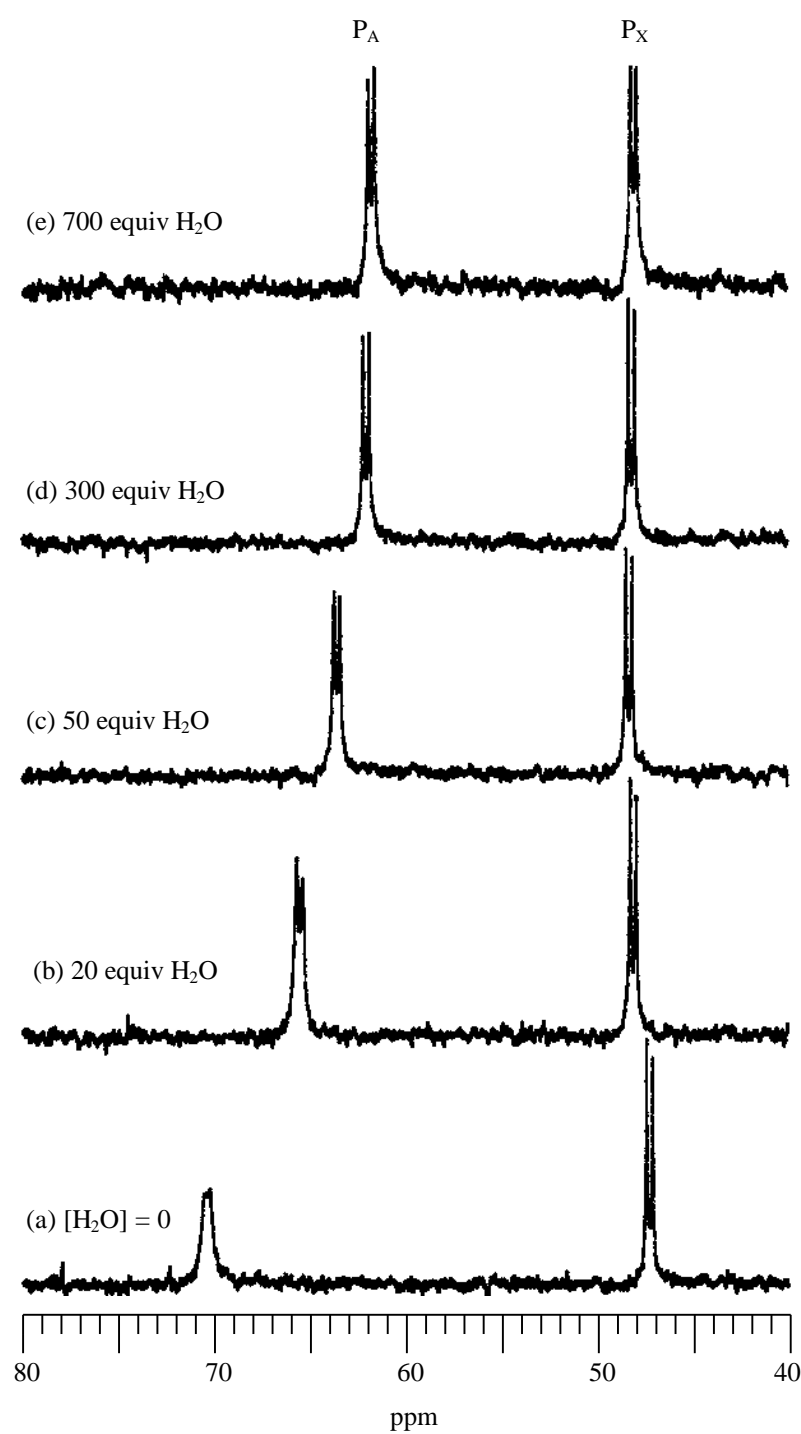


Fig S4 $^{31}\text{P}\{\text{H}\}$ NMR spectra (121.4 MHz, 20 °C) of $\text{RuCl}_2(\text{P}-\text{N})(\text{PPh}_3)$ (**1a**) in d_6 -acetone with added H_2O to form **2a**.

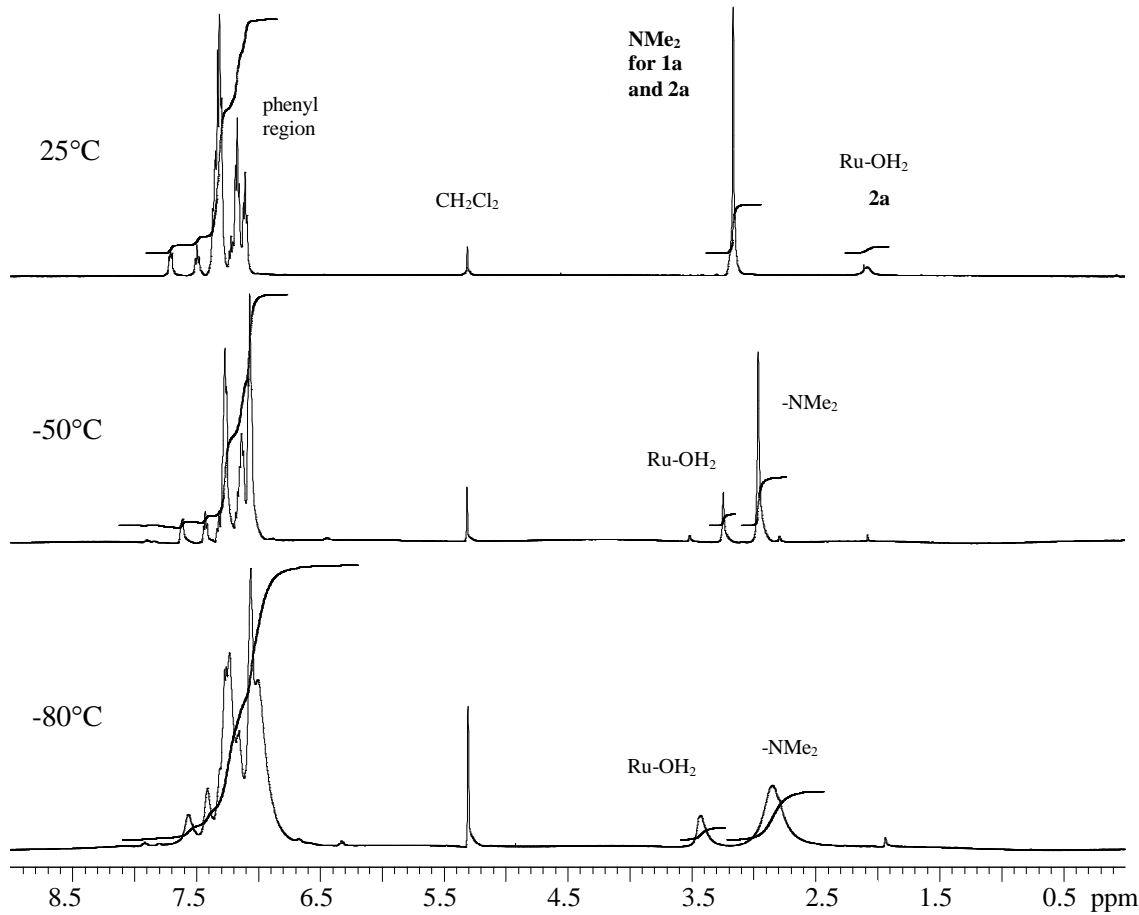


Fig S5 ¹H NMR spectra (500 MHz) of *trans*-RuCl₂(P–N)(PPh₃)(H₂O) (**2a**) in CD_2Cl_2 at various temperatures.

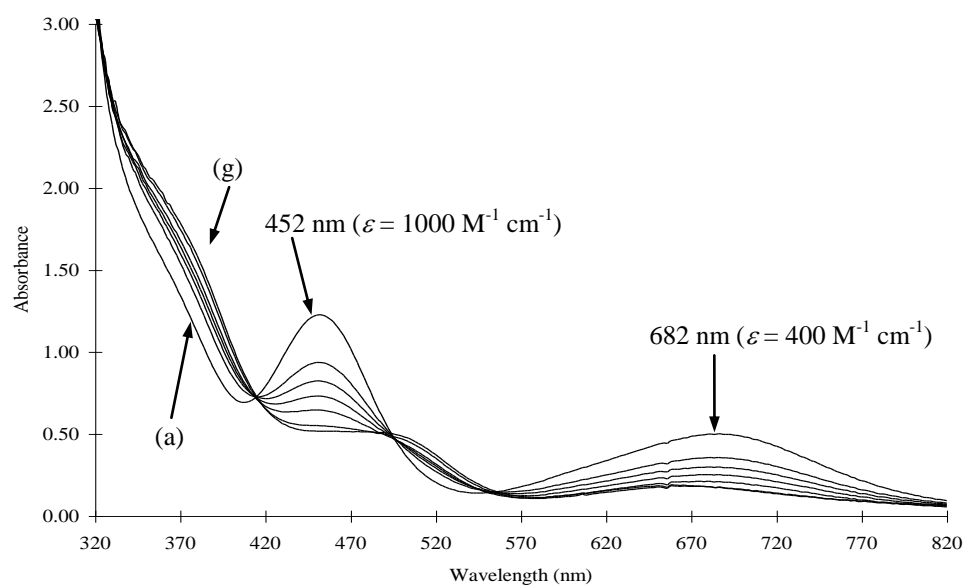


Fig S6 Spectral changes observed upon addition of H_2O to $\text{RuCl}_2(\text{P}-\text{N})(\text{PPh}_3)$ (**1a**) ($1.21 \times 10^{-3} \text{ M}$) in C_6H_6 at 25 °C. Added $[H_2O]$ = (a) 0.0, (b) 0.0056, (c) 0.0111, (d) 0.0222, (e) 0.0333, (f) 0.0444, (g) 0.0776 M.

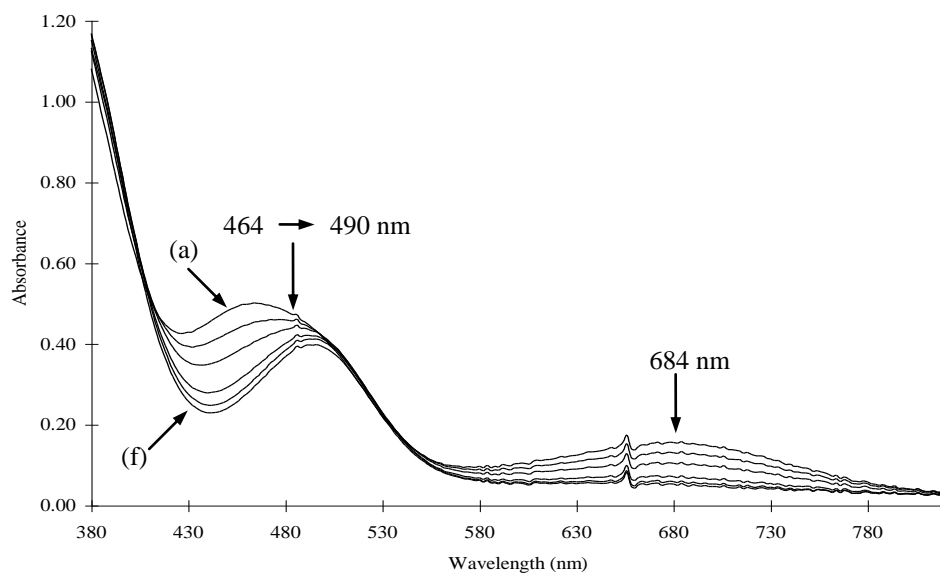


Fig S7 Spectral changes observed upon addition of H_2O to $\text{RuCl}_2(\text{P}-\text{N})(\text{PPh}_3)$ (**1a**) ($1.12 \times 10^{-3} \text{ M}$) in acetone at 25 °C. Added $[H_2O]$ = (a) 0.0, (b) 0.0089, (c) 0.2652, (d) 0.9171, (e) 1.9702, (f) 3.9591 M.

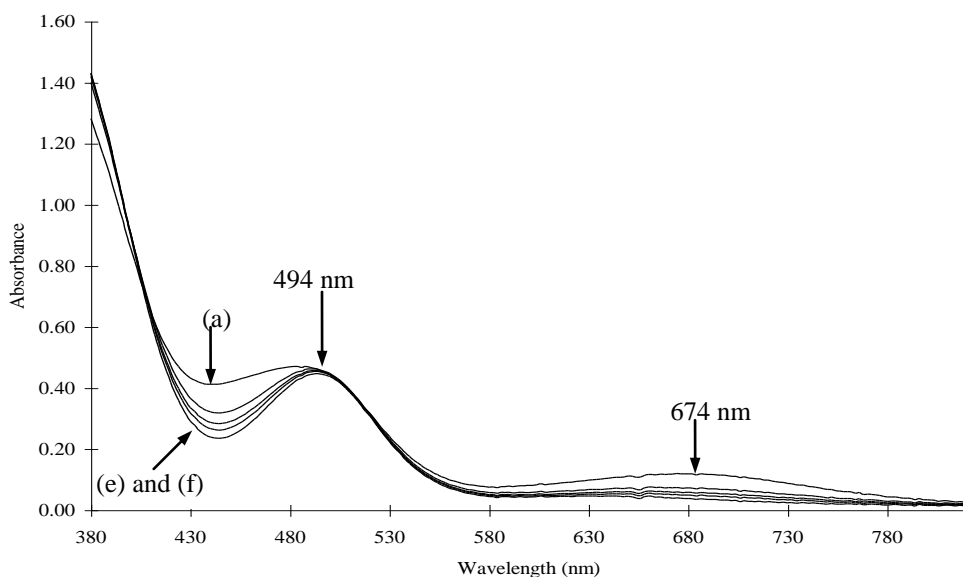


Fig S8 Spectral changes observed upon addition of H₂O to RuCl₂(P–N)(PPh₃) (**1a**) (1.19 × 10⁻³ M) in THF at 25 °C. Added [H₂O] = (a) 0.0, (b) 0.0444, (c) 0.1110, (d) 0.2220, (e) 0.9992, (f) 4.330 M.

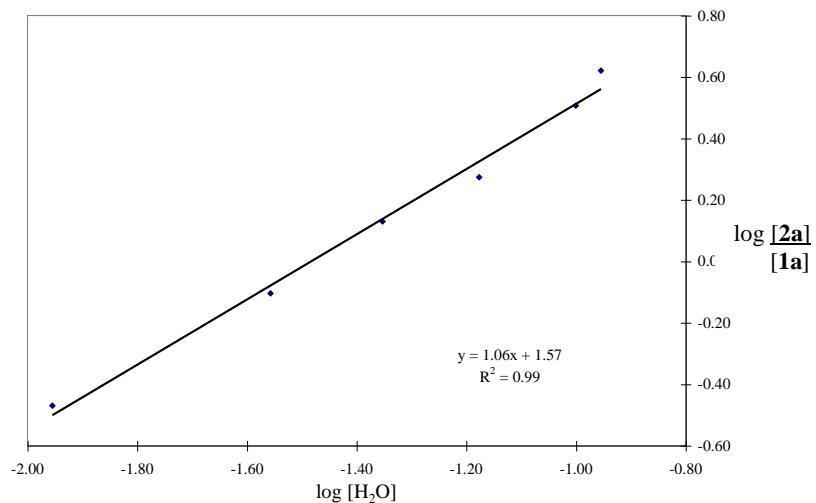


Fig S9 Determination of K for reversible binding of H₂O to **1a** at 25 °C. Concentrations obtained by absorbance at 678 nm (Fig. 4). Data at higher [H₂O] omitted due to solubility limit of H₂O in CH₂Cl₂: 0.128 M at 25 °C (IUPAC Solubility Data Series, Vol. 60, *Halogenerated Methanes with Water*; A. L. Horváth, F. W. Getzen, eds.; Oxford Univ. Press: Oxford, 1995, p. 153).

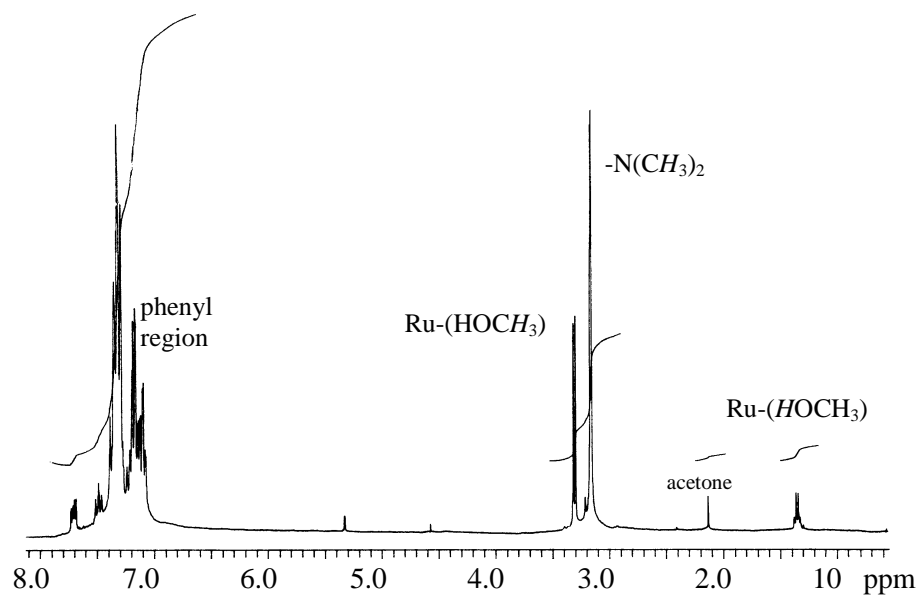


Fig S10 ¹H NMR spectrum (300 MHz) of *trans*-RuCl₂(P–N)(PPh₃)(MeOH) (**3**) in CD₂Cl₂ at room temperature.

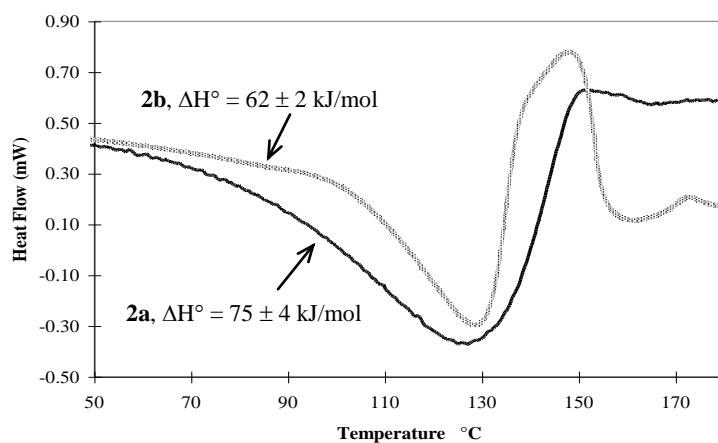


Figure S11. DSC curves for the *trans*-RuCl₂(P–N)(PR₃)(H₂O) complexes **2a** (R = Ph) and **2b** (R = *p*-tolyl).

Table S1 $^{31}\text{P}\{\text{H}\}$ NMR data for $\text{RuCl}_2(\text{P}-\text{N})(\text{PPh}_3)$ (**1a**) and *trans*- $\text{RuCl}_2(\text{P}-\text{N})(\text{PPh}_3)(\text{H}_2\text{O})$ (**2a**) in various solvents at 20 °C.

Solvent	δ_{P_A} ^a		δ_{P_B} ^a		$^2J_{\text{PP}}$ (Hz)	
	1a	2a	1a	2a	1a	2a
CD_2Cl_2	80.51	80.1 br ^b	47.00	48.40 ^b	36.54	37.39 ^b
CDCl_3	83.23	68.5 br ^b	48.41	45.70 ^b	34.82	37.76 ^b
C_6D_6	83.69	73.52 ^b	48.87	49.30 ^b	36.54	38.00 ^b
d_6 -acetone	70.5 br	61.78 ^c	47.27	48.03 ^c	38.36	38.12 ^c

^a All doublets unless specified as br. ^b Data for isolated samples of **2a** in the absence of added H_2O . ^c Data for fully formed **2a** in the presence of added H_2O .

Appendix A

Crystal data for *trans*-RuCl₂(P–N)(P(*p*-tolyl)₃)(OH₂) (**2b**)

Page 3

EXPERIMENTAL

DATA COLLECTION

A red prism crystal of C₄₁H₄₃Cl₂NOP₂Ru having approximate dimensions of 0.100 x 0.180 x 0.200 mm was mounted in a glass capillary. All measurements were made on a Rigaku AFC6S diffractometer with graphite monochromated Cu K α radiation.

Cell constants and an orientation matrix for data collection, obtained from a least-squares refinement using the setting angles of 25 carefully centered reflections in the range 22.26 < 2 θ < 56.17° corresponded to a triclinic cell with dimensions:

$$\begin{array}{ll} a = 11.232 (3)\text{\AA} & \alpha = 102.22 (2)^\circ \\ b = 15.717 (4)\text{\AA} & \beta = 102.91 (2)^\circ \\ c = 11.056 (2)\text{\AA} & \gamma = 86.30 (3)^\circ \\ V = 1858.9 (9)\text{\AA}^3 & \end{array}$$

For Z = 2 and F.W. = 799.72, the calculated density is 1.429 g/cm³. Based on packing considerations, a statistical analysis of intensity distribution, and the successful solution and refinement of the structure, the space group was determined to be:

P\bar{1} (#2)

The data were collected at a temperature of 21 ± 1°C using the ω -2 θ scan technique to a maximum 2 θ value of 155.4°. Omega scans of several intense reflections, made prior to data collection, had an average width at half-height of 0.33° with a take-off angle of 6.0°. Scans of (0.94 + 0.20 tan θ)° were made at a speed of 16.0°/min (in omega). The weak reflections (I < 40.0σ(I)) were rescanned (maximum of 8 rescans) and the counts were accumulated to assure good counting statistics. Stationary background counts were recorded on each side of the reflection. The ratio of peak counting time to background counting time was 2:1. The diameter of the incident beam collimator was 0.5 mm and the crystal to detector distance was 285.0 mm.

DATA REDUCTION

Of the 7989 reflections which were collected, 7573 were unique ($R_{\text{int}} = .039$); equivalent reflections were merged. The intensities of three representative reflections which

Appendix A

Page 4

were measured after every 200 reflections remained constant throughout data collection indicating crystal and electronic stability (no decay correction was applied).

The linear absorption coefficient for Cu K α is 59.3 cm $^{-1}$. An empirical absorption correction, based on azimuthal scans of several reflections, was applied which resulted in transmission factors ranging from 0.68 to 1.00. The data were corrected for Lorentz and polarization effects. A correction for secondary extinction was applied (coefficient = 0.86(5) E-06).

STRUCTURE SOLUTION AND REFINEMENT

The structure was solved by the Patterson method. The non-hydrogen atoms were refined anisotropically. The water hydrogen atoms were refined with isotropic thermal parameters and the remaining hydrogen atoms were fixed in calculated positions with C-H = 0.98 Å.⁴ The final cycle of full-matrix least-squares refinement⁴ was based on 4964 observed reflections ($I > 3.00\sigma(I)$) and 442 variable parameters and converged (largest parameter shift was 0.09 times its esd) with unweighted and weighted agreement factors of:

$$R = \sum |||F_O| - |F_C||| / \sum |F_O| = 0.035$$

$$R_w = [(\sum w (|F_O| - |F_C|)^2 / \sum w F_O^2)]^{1/2} = 0.034$$

The standard deviation of an observation of unit weight⁵ was 1.61. The weighting scheme was based purely on counting statistic ($p = 0.00$). Plots of $\sum w (|F_O| - |F_C|)^2$ versus $|F_O|$, reflection order in data collection, $\sin \theta/\lambda$, and various classes of indices showed no unusual trends. The maximum and minimum peaks on the final difference Fourier map corresponded to 0.34 and -0.45 e $^-/\text{\AA}^3$, respectively.

Neutral atom scattering factors were taken from Cromer and Waber⁶. Anomalous dispersion effects were included in F_{calc} ; the values for $\Delta f'$ and $\Delta f''$ were those of Cromer.⁸ All calculations were performed using the TEXSAN⁹ crystallographic software package of Molecular Structure Corporation.

Appendix A

Page 5

References

- (1) PLUTO:
Motherwell,S. & Clegg,W.; PLUTO. Program for plotting molecular and crystal structures. Univ. of Cambridge, England (1978).
- (2) ORTEP:
Johnson,C.K.; ORTEPII. Report ORNL-5138. Oak Ridge National Laboratory, Oak Ridge, Tennessee (1976).
- (3) Structure Solution Methods:
PHASE
Calbrese,J.C.; PHASE - Patterson Heavy Atom Solution Extractor. Univ. of Wisconsin-Madison, Ph.D. Thesis (1972).
- (4) Least-Squares:
Function minimized: $\sum w ((|Fo| - |Fc|))^2$
where: $w = 4Fo^2 / \sigma^2(Fo^2)$
 $\sigma^2(Fo^2) = [S^2(C+R^2B) + (pFo^2)^2]/Lp^2$
S = Scan rate
C = Total Integrated Peak Count
R = Ratio of Scan Time to background counting time.
B = Total Background Count
Lp = Lorentz-polarization factor
p = p-factor
- (5) Standard deviation of an observation of unit weight:
 $[(\sum w(|Fo| - |Fc|)^2)/(N_o - N_v)]^{1/2}$
where: No = number of observations
Nv = number of variables
- (6) Cromer,D.T. & Waber,J.T.; "International Tables for X-ray Crystallography", Vol. IV, The Kynoch Press, Birmingham, England, Table 2.2 A (1974).
- (7) Ibers,J.A. & Hamilton,W.C.; Acta Crystallogr., 17, 781 (1964).
- (8) D.T. Cromer, "International Tables for X-ray Crystallography", Vol/ IV, The Kynoch Press, Birmingham, England, Table 2.3.1 (1974).
- (9) TEXSAN - TEXRAY Structure Analysis Package, Molecular Structure Corporation (1985).

Appendix A

Page 6

EXPERIMENTAL DETAILS

A. Crystal Data

Empirical Formula	C ₄₁ H ₄₃ Cl ₂ NOP ₂ Ru
Formula Weight	799.72
Crystal Color, Habit	red, prism
Crystal Dimensions (mm)	0.100 x 0.180 x 0.200
Crystal System	triclinic
No. Reflections Used for Unit Cell Determination (2θ range)	25 (22.3 - 56.2°)
Omega Scan Peak Width at Half-height	0.33
Lattice Parameters:	
a =	11.232 (3) Å
b =	15.717 (4) Å
c =	11.056 (2) Å
α =	102.22 (2) °
β =	102.91 (2) °
γ =	86.30 (3) °
v =	1858.9 (9) Å ³
Space Group	P <bar{1}< bar=""> (#2)</bar{1}<>
Z value	2
D _{calc}	1.429 g/cm ³
F ₀₀₀	824
μ (CuKα)	59.26 cm ⁻¹

B. Intensity Measurements

Diffractionometer	Rigaku AFC6S
Radiation	CuKα (λ = 1.54178 Å)
Temperature	21 °C
Take-off Angle	6.0 °

Appendix A

Page 7

Detector Aperture	6.0 mm horizontal 6.0 mm vertical
Crystal to Detector Distance	285 mm
Scan Type	ω -2 θ
Scan Rate	16.0°/min (in omega) (8 rescans)
Scan Width	(0.94 + 0.20 tan θ)°
2 θ _{max}	155.4°
No. of Reflections Measured	Total: 7989 Unique: 7573 (R_{int} = .039)
Corrections	Lorentz-polarization Absorption (trans. factors: 0.68 - 1.00) Secondary Extinction (coefficient: 0.86(5) E-06)

C. Structure Solution and Refinement

Structure Solution	Patterson Method
Refinement	Full-matrix least-squares
Function Minimized	$\Sigma w (F_o - F_c)^2$
Least-squares Weights	$4F_o^2/\sigma^2(F_o^2)$
p-factor	0.00
Anomalous Dispersion	All non-hydrogen atoms
No. Observations ($I > 3.00\sigma(I)$)	4964
No. Variables	442
Reflection/Parameter Ratio	11.23
Residuals: R; R _w	0.035; 0.034
Goodness of Fit Indicator	1.61
Max Shift/Error in Final Cycle	0.09
Maximum Peak in Final Diff. Map	$0.34 e^-/\text{\AA}^3$
Minimum Peak in Final Diff. Map	$-0.45 e^-/\text{\AA}^3$

Appendix A

Table . Final atomic coordinates (fractional) and B_{eq} (\AA^2)*

atom	x	y	z	B_{eq}
Ru(1)	0.05149(3)	0.21639(2)	0.07921(3)	3.03(1)
Cl(1)	0.11309(10)	0.08469(7)	0.15857(10)	4.01(4)
Cl(2)	-0.01142(11)	0.31700(8)	-0.05781(9)	4.51(5)
P(1)	0.15569(10)	0.29625(7)	0.25700(9)	3.07(4)
P(2)	-0.13618(10)	0.23037(7)	0.12966(10)	3.22(4)
O(1)	-0.0200(4)	0.1202(3)	-0.1012(3)	4.5(2)
N(1)	0.2451(3)	0.2047(2)	0.0340(3)	3.6(1)
C(1)	0.3072(3)	0.2444(3)	0.2659(4)	3.3(2)
C(2)	0.3346(4)	0.2000(3)	0.1524(4)	3.5(2)
C(3)	0.4456(4)	0.1565(3)	0.1517(4)	4.3(2)
C(4)	0.5279(4)	0.1551(3)	0.2653(5)	4.9(2)
C(5)	0.5014(4)	0.1985(4)	0.3774(5)	5.2(2)
C(6)	0.3926(4)	0.2440(3)	0.3781(4)	4.6(2)
C(7)	0.1182(4)	0.2938(3)	0.4083(3)	3.4(2)
C(8)	0.0559(4)	0.3644(3)	0.4675(4)	4.4(2)
C(9)	0.0256(5)	0.3616(4)	0.5814(5)	5.7(3)
C(10)	0.0541(5)	0.2904(4)	0.6350(4)	5.7(3)
C(11)	0.1135(5)	0.2202(4)	0.5762(4)	5.4(2)
C(12)	0.1436(4)	0.2204(3)	0.4604(4)	4.4(2)
C(13)	0.1996(4)	0.4119(3)	0.2841(4)	3.7(2)
C(14)	0.2715(5)	0.4508(3)	0.3994(4)	5.2(2)
C(15)	0.3124(5)	0.5345(4)	0.4170(5)	6.1(3)
C(16)	0.2862(5)	0.5791(3)	0.3209(7)	6.3(3)
C(17)	0.2152(5)	0.5418(3)	0.2076(6)	5.5(2)
C(18)	0.1718(4)	0.4583(3)	0.1874(4)	4.2(2)

Appendix A

Table . Final atomic coordinates (fractional) and B_{eq} (\AA^2)* (cont.)

atom	x	y	z	B_{eq}
C(19)	0.2486(4)	0.1256(3)	-0.0651(4)	5.0(2)
C(20)	0.2802(4)	0.2781(3)	-0.0138(4)	4.8(2)
C(21)	-0.1550(4)	0.1776(3)	0.2571(4)	3.3(2)
C(22)	-0.1800(4)	0.2259(3)	0.3706(4)	3.8(2)
C(23)	-0.1880(4)	0.1850(3)	0.4681(4)	4.0(2)
C(24)	-0.1733(4)	0.0956(3)	0.4572(4)	4.1(2)
C(25)	-0.1375(4)	0.0883(3)	0.2477(4)	3.5(2)
C(26)	-0.1481(4)	0.0483(3)	0.3447(4)	3.9(2)
C(27)	-0.1831(5)	0.0524(4)	0.5638(4)	5.9(3)
C(28)	-0.2590(4)	0.1849(3)	-0.0081(4)	3.5(2)
C(29)	-0.3052(5)	0.1050(3)	-0.0301(5)	5.3(2)
C(30)	-0.3957(5)	0.0743(3)	-0.1372(5)	6.0(2)
C(31)	-0.4413(4)	0.1244(3)	-0.2246(4)	4.3(2)
C(32)	-0.3949(5)	0.2047(4)	-0.2030(5)	5.8(2)
C(33)	-0.3042(5)	0.2349(3)	-0.0981(5)	5.7(2)
C(34)	-0.5408(5)	0.0906(4)	-0.3388(5)	6.4(3)
C(35)	-0.2082(4)	0.3375(3)	0.1691(4)	3.6(2)
C(36)	-0.3287(4)	0.3439(3)	0.1836(5)	4.5(2)
C(37)	-0.3892(4)	0.4233(3)	0.2016(5)	5.1(2)
C(38)	-0.3323(5)	0.4996(3)	0.2047(5)	5.0(2)
C(39)	-0.2134(5)	0.4933(3)	0.1896(5)	4.7(2)
C(40)	-0.1514(4)	0.4140(3)	0.1739(4)	4.0(2)
C(41)	-0.3986(6)	0.5864(4)	0.2219(7)	7.8(3)

$$*B_{eq} = (8/3)\pi^2 \sum \sum U_{ij} a_i * a_j * (a_i \cdot a_j)$$

Appendix A

Hydrogen atom coordinates (fractional) and B_{iso} (\AA^2)

atom	x	y	z	B_{iso}
H(1)	-0.044(6)	0.067(4)	-0.086(6)	11(2)
H(2)	-0.069(6)	0.141(4)	-0.133(6)	9(2)
H(3)	0.4659	0.1267	0.0714	5.1
H(4)	0.6055	0.1228	0.2652	5.8
H(5)	0.5600	0.1973	0.4573	6.3
H(6)	0.3752	0.2764	0.4584	5.5
H(7)	0.0340	0.4155	0.4289	5.2
H(8)	-0.0171	0.4114	0.6239	6.8
H(9)	0.0323	0.2894	0.7157	6.9
H(10)	0.1350	0.1695	0.6158	6.5
H(11)	0.1825	0.1690	0.4166	5.2
H(12)	0.2933	0.4189	0.4685	6.3
H(13)	0.3610	0.5621	0.4997	7.4
H(14)	0.3181	0.6376	0.3333	7.5
H(15)	0.1946	0.5745	0.1391	6.7
H(16)	0.1215	0.4321	0.1050	5.1
H(17)	0.2262	0.0751	-0.0364	6.0
H(18)	0.1908	0.1325	-0.1432	6.0
H(19)	0.3313	0.1166	-0.0813	6.0
H(20)	0.3629	0.2677	-0.0295	5.8
H(21)	0.2227	0.2834	-0.0929	5.8
H(22)	0.2782	0.3321	0.0494	5.8
H(23)	-0.1918	0.2892	0.3814	4.5
H(24)	-0.2047	0.2204	0.5470	4.8
H(25)	-0.1171	0.0528	0.1705	4.2

Appendix A

Hydrogen atom coordinates (fractional) and B_{iso} (\AA^2) (cont.)

atom	x	y	z	B_{iso}
H(26)	-0.1376	-0.0151	0.3335	4.7
H(27)	-0.2643	0.0646	0.5833	7.0
H(28)	-0.1711	-0.0106	0.5385	7.0
H(29)	-0.1205	0.0752	0.6391	7.0
H(30)	-0.2747	0.0673	0.0307	6.4
H(31)	-0.4270	0.0156	-0.1499	7.2
H(32)	-0.4264	0.2426	-0.2634	7.0
H(33)	-0.2711	0.2929	-0.0872	6.8
H(34)	-0.5667	0.0336	-0.3329	7.7
H(35)	-0.6107	0.1314	-0.3415	7.7
H(36)	-0.5095	0.0850	-0.4161	7.7
H(37)	-0.3714	0.2909	0.1809	5.4
H(38)	-0.4736	0.4257	0.2125	6.1
H(39)	-0.1717	0.5463	0.1899	5.6
H(40)	-0.0661	0.4121	0.1660	4.8
H(41)	-0.4666	0.5871	0.1491	9.4
H(42)	-0.3420	0.6329	0.2285	9.4
H(43)	-0.4303	0.5956	0.2995	9.4

Appendix A

Table . Selected bond lengths (Å) and angles (°).

atom	atom	distance	atom	atom	distance		
Ru(1)	Cl(1)	2.418(1)	P(1)	C(13)	1.859(4)		
Ru(1)	Cl(2)	2.385(1)	P(2)	C(21)	1.835(4)		
Ru(1)	P(1)	2.220(1)	P(2)	C(28)	1.861(4)		
Ru(1)	P(2)	2.284(1)	P(2)	C(35)	1.831(4)		
Ru(1)	O(1)	2.252(4)	N(1)	C(2)	1.474(5)		
Ru(1)	N(1)	2.326(4)	N(1)	C(19)	1.477(5)		
P(1)	C(1)	1.830(4)	N(1)	C(20)	1.475(5)		
P(1)	C(7)	1.822(4)	atom	atom	angle		
Cl(1)	Ru(1)	Cl(2)	162.91(4)	Ru(1)	P(1)	C(13)	127.2(1)
Cl(1)	Ru(1)	P(1)	90.73(4)	C(1)	P(1)	C(7)	104.5(2)
Cl(1)	Ru(1)	P(2)	96.26(5)	C(1)	P(1)	C(13)	99.3(2)
Cl(1)	Ru(1)	O(1)	82.2(1)	C(7)	P(1)	C(13)	100.6(2)
Cl(1)	Ru(1)	N(1)	83.7(1)	Ru(1)	P(2)	C(21)	116.7(1)
Cl(2)	Ru(1)	P(1)	104.30(5)	Ru(1)	P(2)	C(28)	111.9(1)
Cl(2)	Ru(1)	P(2)	89.74(5)	Ru(1)	P(2)	C(35)	121.2(2)
Cl(2)	Ru(1)	O(1)	81.6(1)	C(21)	P(2)	C(28)	104.8(2)
Cl(2)	Ru(1)	N(1)	90.8(1)	C(21)	P(2)	C(35)	102.7(2)
P(1)	Ru(1)	P(2)	98.04(5)	C(28)	P(2)	C(35)	96.7(2)
P(1)	Ru(1)	O(1)	168.8(1)	Ru(1)	N(1)	C(2)	107.7(2)
P(1)	Ru(1)	N(1)	80.20(9)	Ru(1)	N(1)	C(19)	107.8(3)
P(2)	Ru(1)	O(1)	91.4(1)	Ru(1)	N(1)	C(20)	115.3(3)
P(2)	Ru(1)	N(1)	178.24(9)	C(2)	N(1)	C(19)	112.1(3)
O(1)	Ru(1)	N(1)	90.3(1)	C(2)	N(1)	C(20)	106.9(3)
Ru(1)	P(1)	C(1)	101.1(1)	C(19)	N(1)	C(20)	107.1(3)
Ru(1)	P(1)	C(7)	120.1(1)				

Appendix A

Table . Bond lengths (Å) with estimated standard deviations.

atom	atom	distance	atom	atom	distance
Ru(1)	Cl(1)	2.418(1)	C(13)	C(14)	1.387(6)
Ru(1)	Cl(2)	2.385(1)	C(13)	C(18)	1.387(5)
Ru(1)	P(1)	2.220(1)	C(14)	C(15)	1.382(6)
Ru(1)	P(2)	2.284(1)	C(15)	C(16)	1.363(7)
Ru(1)	O(1)	2.252(4)	C(16)	C(17)	1.361(7)
Ru(1)	N(1)	2.326(4)	C(17)	C(18)	1.386(6)
P(1)	C(1)	1.830(4)	C(21)	C(22)	1.398(5)
P(1)	C(7)	1.822(4)	C(21)	C(25)	1.391(5)
P(1)	C(13)	1.859(4)	C(22)	C(23)	1.390(6)
P(2)	C(21)	1.835(4)	C(23)	C(24)	1.387(6)
P(2)	C(28)	1.861(4)	C(24)	C(26)	1.385(6)
P(2)	C(35)	1.831(4)	C(24)	C(27)	1.506(6)
N(1)	C(2)	1.474(5)	C(25)	C(26)	1.383(5)
N(1)	C(19)	1.477(5)	C(28)	C(29)	1.344(6)
N(1)	C(20)	1.475(5)	C(28)	C(33)	1.385(6)
C(1)	C(2)	1.390(5)	C(29)	C(30)	1.397(6)
C(1)	C(6)	1.389(5)	C(30)	C(31)	1.365(6)
C(2)	C(3)	1.383(6)	C(31)	C(32)	1.351(6)
C(3)	C(4)	1.386(6)	C(31)	C(34)	1.512(6)
C(4)	C(5)	1.368(7)	C(32)	C(33)	1.382(6)
C(5)	C(6)	1.376(6)	C(35)	C(36)	1.393(6)
C(7)	C(8)	1.395(6)	C(35)	C(40)	1.383(6)
C(7)	C(12)	1.381(6)	C(36)	C(37)	1.380(6)
C(8)	C(9)	1.386(6)	C(37)	C(38)	1.387(6)
C(9)	C(10)	1.362(7)	C(38)	C(39)	1.377(6)
C(10)	C(11)	1.371(7)	C(38)	C(41)	1.507(6)
C(11)	C(12)	1.396(6)	C(39)	C(40)	1.385(6)

Appendix B. Thermodynamic calculations and UV-Vis spectroscopic data for the reversible formation of *trans*-RuCl₂(P–N)(PR₃)(H₂O).

NOTE: The complexes numbered **1a** and **2a** in the manuscript are here labelled **6a** and **33a**, respectively, and the Tables are numbered **XII.1.1–XII.1.9**, and **XII.2.1**.

**Thermodynamic Calculations and Data for the Reversible Formation of
Trans-RuCl₂(P-N)(PPh₃)(OH₂) (33a) (UV-Vis Spectroscopic Data)**

For the equilibrium:



$$K = \frac{[\text{33a}]}{[\text{6a}][\text{H}_2\text{O}]} \quad (2)$$

$$\log\left(\frac{[\text{33a}]}{[\text{6a}]}\right) = \log K + n \log[\text{H}_2\text{O}] \quad (3)$$

where $n = 1$ (slope)

plot of $\log\left(\frac{[\text{33a}]}{[\text{6a}]}\right)$ versus $\log [\text{H}_2\text{O}]$ gives intercept = $\log K$

$$A = \epsilon c \ell \quad (4)$$

where A=absorbance

ϵ = molar absorptivity ($\text{M}^{-1} \text{cm}^{-1}$)

c = concentration (M)

ℓ = pathlength = 1 cm

$$A = A_{\text{6a}} + A_{\text{33a}} = \epsilon_{\text{6a}}[\text{6a}] + \epsilon_{\text{33a}}[\text{33a}] \quad (5)$$

$$[\text{Ru}]_{\text{total}} = [\text{6a}] + [\text{33a}] \quad (6)$$

$$\epsilon_{\text{6a}} = \frac{A_0}{[\text{Ru}]_{\text{total}}} \quad (7)$$

$$\epsilon_{\text{33a}} = \frac{A_\infty}{[\text{Ru}]_{\text{total}}} \quad (8)$$

Solve for [6a] and [33a] by substitution of equations (6) and (7) into (5), and equations (6) and (8) into (5), respectively:

$$\left| \frac{[\text{33a}]}{[\text{6a}]} \right| = \left| \frac{A - A_0}{A - A_\infty} \right| \quad (9)$$

XII.1 Calculations in CH₂Cl₂

Trial 1 at 25°C

Table XII.1.1 Calculation of K at T = 25°C; 5.2 × 10⁻⁶ mol **6a** dissolved in 5.0 mL CH₂Cl₂ ([Ru]_{total} = 1.04 × 10⁻³ M); absorbances monitored at λ_{\max} = 678 nm; A₀ = 0.52, A_∞ = 0.078 (estimated from a flat baseline between λ = 550 to 820 nm).

H ₂ O added (μL)	[H ₂ O] (M)	log [H ₂ O]	A at λ_{\max} = 678 nm	$\frac{[33a]}{[6a]}$	log $\frac{[33a]}{[6a]}$
0.0	0.0000	-	0.52	-0.00052	-
0.5	0.0056	-2.26	0.47	0.11119	-0.95
1.0	0.0111	-1.95	0.41	0.33838	-0.47
2.5	0.0278	-1.56	0.33	0.78687	-0.10
4.0	0.0444	-1.35	0.27	1.34657	0.13
6.0	0.0666	-1.18	0.23	1.87686	0.27
9.0	0.0999	-1.00	0.18	3.21073	0.51
10.0	0.1110	-0.95	0.16	4.17443	0.62
17.0	0.1887	-0.72	0.15	5.22535	0.72

Plot of plot of $\log(\frac{[33a]}{[6a]})$ versus log [H₂O] (see Figure 59) gives y = 1.06x + 1.57; K = 37 M⁻¹.

Trial 2 at 25°C

Table XII.1.2 Calculation of K at T = 25°C; 3.0 × 10⁻⁶ mol **6a** dissolved in 5.0 mL CH₂Cl₂ ([Ru]_{total} = 6.0 × 10⁻⁴ M); absorbances monitored at λ_{\max} = 678 nm; A₀ = 0.30, A_∞ = 0.045 (estimated from a flat baseline between λ = 550 to 820 nm).

H ₂ O added (μL)	[H ₂ O] (M)	log [H ₂ O]	A at λ_{\max} = 678 nm	$\frac{[33a]}{[6a]}$	log $\frac{[33a]}{[6a]}$
0.0	0.0000	-	0.30	0.00252	-2.60
0.1	0.0006	-3.26	0.25	0.26758	-0.57
1.0	0.0111	-1.95	0.20	0.69199	-0.16
1.5	0.0167	-1.78	0.15	1.46377	0.17
3.5	0.0389	-1.41	0.12	2.40864	0.38
6.5	0.0722	-1.14	0.10	3.54626	0.55
8.5	0.0944	-1.03	0.09	5.07432	0.71
12.0	0.1332	-0.88	0.08	6.55556	0.82
17.0	0.1887	-0.72	0.08	6.92910	0.84

Plot of plot of $\log(\frac{[33a]}{[6a]})$ versus log [H₂O] gives y = 0.83x + 1.54; K = 35 M⁻¹.

Trial 1 at 10°C

Table XII.1.3 Calculation of K at T = 10°C; 4.0×10^{-6} mol **6a** dissolved in 5.0 mL CH₂Cl₂ ($[\text{Ru}]_{\text{total}} = 8.1 \times 10^{-4}$ M); absorbances monitored at $\lambda_{\text{max}} = 678$ nm; $A_0 = 0.39$, $A_\infty = 0.07$ (estimated from a flat baseline between $\lambda = 550$ to 820 nm).

H ₂ O added (μL)	[H ₂ O] (M)	log [H ₂ O]	A at $\lambda_{\text{max}} = 678$ nm	$\frac{[33\text{a}]}{[6\text{a}]}$	log $\frac{[33\text{a}]}{[6\text{a}]}$
0.0	0.0000	-	0.39	0.00000	-
0.5	0.0056	-2.26	0.35	0.14286	-0.85
1.0	0.0111	-1.95	0.31	0.33333	-0.48
1.5	0.0167	-1.78	0.27	0.60000	-0.22
2.0	0.0222	-1.65	0.25	0.77778	-0.11
3.0	0.0333	-1.48	0.21	1.28571	0.11
4.0	0.0444	-1.35	0.20	1.46154	0.16
6.0	0.0666	-1.18	0.18	1.90909	0.28

Plot of plot of $\log(\frac{[33\text{a}]}{[6\text{a}]})$ versus log [H₂O] gives $y = 1.07x + 1.62$; $K = 42$ M⁻¹.

Trial 2 at 10°C

Table XII.1.4 Calculation of K at T = 10°C; 4.1×10^{-6} mol **6a** dissolved in 5.0 mL CH₂Cl₂ ($[\text{Ru}]_{\text{total}} = 8.2 \times 10^{-4}$ M); absorbances monitored at $\lambda_{\text{max}} = 678$ nm; $A_0 = 0.40$, $A_\infty = 0.07$ (estimated from a flat baseline between $\lambda = 550$ to 820 nm).

H ₂ O added (μL)	[H ₂ O] (M)	log [H ₂ O]	A at $\lambda_{\text{max}} = 678$ nm	$\frac{[33\text{a}]}{[6\text{a}]}$	log $\frac{[33\text{a}]}{[6\text{a}]}$
0.0	0.0000	-	0.40	0.00000	-
0.5	0.0056	-2.26	0.34	0.22222	-0.65
1.0	0.0111	-1.95	0.30	0.43478	-0.36
1.5	0.0167	-1.78	0.25	0.83333	-0.08
2.0	0.0222	-1.65	0.22	1.20000	0.08
3.0	0.0333	-1.48	0.19	1.75000	0.24
4.0	0.0444	-1.35	0.16	2.66667	0.43
6.0	0.0666	-1.18	0.12	5.60000	0.75

Plot of plot of $\log(\frac{[33\text{a}]}{[6\text{a}]})$ versus log [H₂O] gives $y = 1.28x + 2.18$; $K = 151$ M⁻¹.

Trial 1 at 35°C

Table XII.1.5 Calculation of K at T = 35°C; 4.5×10^{-6} mol **6a** dissolved in 5.0 mL CH₂Cl₂ ([Ru]_{total} = 9.0×10^{-4} M); absorbances monitored at $\lambda_{\max} = 678$ nm; A₀ = 0.43, A_∞ = 0.08 (estimated from a flat baseline between $\lambda = 550$ to 820 nm).

H ₂ O added (μL)	[H ₂ O] (M)	log [H ₂ O]	A at $\lambda_{\max} = 678$ nm	$\frac{[33a]}{[6a]}$	log $\frac{[33a]}{[6a]}$
0.0	0.0000	-	0.42	0.02609	-
1.0	0.0111	-1.95	0.34	0.32180	-0.49
2.0	0.0222	-1.65	0.30	0.60860	-0.22
3.0	0.0333	-1.48	0.25	1.08694	0.04
4.0	0.0444	-1.35	0.23	1.37176	0.14
6.0	0.0666	-1.18	0.21	1.60359	0.21
9.0	0.0999	-1.00	0.20	1.91569	0.28
12.0	0.1332	-0.88	0.19	2.14861	0.33

Plot of plot of $\log(\frac{[33a]}{[6a]})$ versus log [H₂O] gives y = 0.84x + 1.20; K = 16 M⁻¹.

Trial 2 at 35°C

Table XII.1.6 Calculation of K at T = 35°C; 4.8×10^{-6} mol **6a** dissolved in 5.0 mL CH₂Cl₂ ([Ru]_{total} = 9.7×10^{-4} M); absorbances monitored at $\lambda_{\max} = 678$ nm; A₀ = 0.43, A_∞ = 0.075 (estimated from a flat baseline between $\lambda = 550$ to 820 nm).

H ₂ O added (μL)	[H ₂ O] (M)	log [H ₂ O]	A at $\lambda_{\max} = 678$ nm	$\frac{[33a]}{[6a]}$	log $\frac{[33a]}{[6a]}$
0.0	0.0000	-	0.43	-0.00591	-
1.0	0.0111	-1.95	0.37	0.20433	-0.69
2.0	0.0222	-1.65	0.32	0.43649	-0.36
3.0	0.0333	-1.48	0.28	0.70044	-0.15
4.0	0.0444	-1.35	0.26	0.94755	-0.02
6.0	0.0666	-1.18	0.23	1.36100	0.13
9.0	0.0999	-1.00	0.20	1.89962	0.28
12.0	0.1332	-0.88	0.19	2.12886	0.33

Plot of plot of $\log(\frac{[33a]}{[6a]})$ versus log [H₂O] gives y = 1.03x + 1.34; K = 22 M⁻¹.

Trial 1 at 38°C

Table XII.1.7 Calculation of K at T = 38°C; 5.4×10^{-6} mol **6a** dissolved in 5.0 mL CH₂Cl₂ ([Ru]_{total} = 1.08×10^{-3} M); absorbances monitored at $\lambda_{\max} = 678$ nm; A₀ = 0.48, A_∞ = 0.08 (estimated from a flat baseline between $\lambda = 550$ to 820 nm).

H ₂ O added (μL)	[H ₂ O] (M)	log [H ₂ O]	A at $\lambda_{\max} = 678$ nm	$\frac{[33a]}{[6a]}$	log $\frac{[33a]}{[6a]}$
0.0	0.0000	-	0.48	0.00000	-
1.0	0.0111	-1.95	0.37	0.37931	-0.42
2.0	0.0222	-1.65	0.34	0.53846	-0.27
3.0	0.0333	-1.48	0.27	1.10526	0.04
5.0	0.0555	-1.26	0.25	1.35294	0.13
7.0	0.0777	-1.11	0.22	1.85714	0.27
10.0	0.1110	-0.95	0.18	3.00000	0.48
12.0	0.1332	-0.88	0.15	4.71429	0.67

Plot of plot of $\log(\frac{[33a]}{[6a]})$ versus log [H₂O] gives $y = 0.89x + 1.29$; K = 20 M⁻¹.

Trial 2 at 38°C

Table XII.1.8 Calculation of K at T = 38°C; 6.2×10^{-6} mol **6a** dissolved in 5.0 mL CH₂Cl₂ ([Ru]_{total} = 1.25×10^{-3} M); absorbances monitored at $\lambda_{\max} = 678$ nm; A₀ = 0.60, A_∞ = 0.085 (estimated from a flat baseline between $\lambda = 550$ to 820 nm).

H ₂ O added (μL)	[H ₂ O] (M)	log [H ₂ O]	A at $\lambda_{\max} = 678$ nm	$\frac{[33a]}{[6a]}$	log $\frac{[33a]}{[6a]}$
0.0	0.0000	-	0.60	0.00000	-
1.0	0.0111	-1.95	0.55	0.10753	-0.97
2.0	0.0222	-1.65	0.47	0.33766	-0.47
3.0	0.0333	-1.48	0.44	0.45070	-0.35
5.0	0.0555	-1.26	0.39	0.68852	-0.16
7.0	0.0777	-1.11	0.38	0.74576	-0.13
10.0	0.1110	-0.95	0.37	0.80702	-0.09
12.0	0.1332	-0.88	0.36	0.87273	-0.06

Plot of plot of $\log(\frac{[33a]}{[6a]})$ versus log [H₂O] gives $y = 0.78x + 0.70$; K = 5 M⁻¹.

Table XII.1.9 Equilibrium constants for the reversible formation of **33a** at various temperatures (K obtained from Tables XII.1.1 - XII.1.9).

Temp (°C)	1/T (K)	K	ln K
10	0.003532	42	3.74
10	0.003532	151	5.02
25	0.003354	37	3.61
25	0.003354	35	3.56
35	0.003245	16	2.77
35	0.003245	22	3.09
38	0.003214	20	3.00
38	0.003214	5	1.61

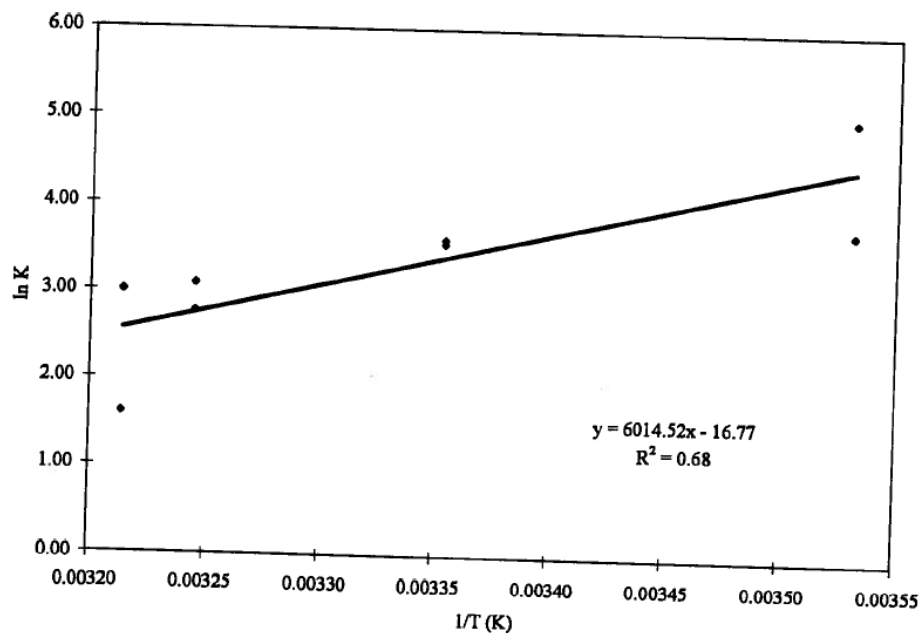


Figure XII.1 Van't Hoff plot for the reversible formation of $\text{RuCl}_2(\text{P-N})(\text{PPh}_3)(\text{OH}_2)$ **33a**.

Estimated thermodynamic parameters from the above plot are:
 $\Delta H^\circ = -50 \pm 20 \text{ kJ/mol}$; $\Delta S^\circ = -140 \pm 40 \text{ J/mol K}$; $\Delta G^\circ = -8.9 \pm 0.2 \text{ kJ/mol}$ (25°C , based on $K = 37 \pm 2 \text{ M}^{-1}$).

XII.2 Calculations in C₆H₆

Table XII.2.1 Calculation of K at T = 25°C; 6.0 × 10⁻⁶ mol **6a** dissolved in 5.0 mL C₆H₆ ([Ru]_{total} = 1.20 × 10⁻³ M); absorbances monitored at $\lambda_{\text{max}} = 682 \text{ nm}$; A₀ = 0.50, A_∞ = 0.090 (estimated from a flat baseline between $\lambda = 550$ to 820 nm).

H ₂ O added (μL)	[H ₂ O] (M)	log [H ₂ O]	A at $\lambda_{\text{max}} = 682 \text{ nm}$	$\frac{[33a]}{[6a]}$	log $\frac{[33a]}{[6a]}$
0.0	0.0	-	0.50	0.00001	-5.00
0.5	0.0056	-2.26	0.35	0.50333	-0.30
1.0	0.0111	-1.95	0.30	0.88328	-0.05
2.0	0.0222	-1.65	0.25	1.37334	0.14
3.0	0.0333	-1.48	0.21	2.08413	0.32
4.0	0.0444	-1.35	0.18	3.04990	0.48
7.0	0.0776	-1.11	0.17	3.4629	0.54

Plot of plot of $\log(\frac{[33a]}{[6a]})$ versus log [H₂O] gives y = 0.77x + 1.45; K = 28 M⁻¹.*

*Determination of K in C₆H₆ is more difficult and less accurate than in CH₂Cl₂ because water has a lower solubility in C₆H₆ (0.0356 M, 25°C)¹ than in CH₂Cl₂ (0.128 M, 25°C).²

1. IUPAC Solubility Data Series, Volume 37, Hydrocarbons with Water and Seawater Part I: Hydrocarbons C₅ to C₇; Kertes, A. S., Ed. Pergamon Press: Toronto, 1989, p. 95.
2. IUPAC Solubility Data Series, Volume 60, Halogenated Methanes with Water; Horváth, A. L.; Getzen, F. W., Eds.; Oxford University Press: Oxford, 1995, p. 153.